Calibration of magnitude error of lock-in amplifiers and noise response

(Article begins on next page)

Calibration of Magnitude Error of Lock-in Amplifiers and Noise Response

Alessandro Cultrera[1], Juan Medved[1, 2], Massimo Ortolano[2], Paolo Durandetto[1],
Andrea Sosso[1] and Luca Callegaro[1]
[1] Istituto Nazionale di Ricerca Metrologica (INRIM), Torino, Italy
a.cultrera@inrim.it
[2]Department of Electronics and Telecommunications, Politecnico di Torino, Torino, Italy

***Abstract*—In this work the calibration of the magnitude error and the noise response of a digital lock-in amplifier are presented. A simple but effective calibration setup developed at INRIM is used to assess the magnitude error of a recent model of lock-in amplifier. The noise response of the instrument is analyzed in terms of Allan deviation for different filter orders.**

***Index Terms*—Metrology, signal detection, noise measurement, digital filters, calibration.**

I. Introduction

Lock-in amplifiers (LIAs) are the most popular signal recovery instruments. They are employed in countless physics and engineering laboratory experiments involving small electrical signals. A number of measurement setups use LIAs as small voltage (or current) vector meters, the instrument reading being related to the value of the physical quantity of interest. The specified base accuracy of a commercial LIA is typically around $1\,\%$, which can have a significant impact on the measurement uncertainty of the quantity of interest. A calibration of the instrument, and the characterisation of its noise response, is the proper route to improve the overall measurement accuracy and the evaluation of the uncertainty. In recent years, National Metrology Institutes have been developing techniques [1]–[3] for the traceable calibration of the magnitude error of LIAs in the voltage reading mode. In 2020, INRIM and METAS performed an inter-comparison [2], [4] to mutually validate their calibration capabilities. A popular LIA model [5], available since the 1990s, was employed as transfer standard. In this work, we describe the progress made on the characterisation of LIAs. The focus is on a more recent instrument model, a Zurich Instruments (ZI) MFLI $500\,\mathrm{kHz}$, with the determination of its magnitude error in presence of a phase shift between the calibration signal and the reference signal, and of the instrument noise response as a function of its low-pass filter order.

II. Magnitude Error

The LIA under test (DUT) has a specified input gain accuracy within $1\,\%$ [6]; the lowest input voltage range is $1\,\mathrm{mV}$. To assess the DUT magnitude error, a reference signal and a calibration signal are generated by a two-channel AC digital voltage source [7]. The reference signal REF is generated by channel 2. Channel 1 generates a large and stable sinusoidal signal V_{S} with a nominal RMS value of $1\,\mathrm{V}$ which is then scaled down by an inductive voltage divider (IVD) cascaded

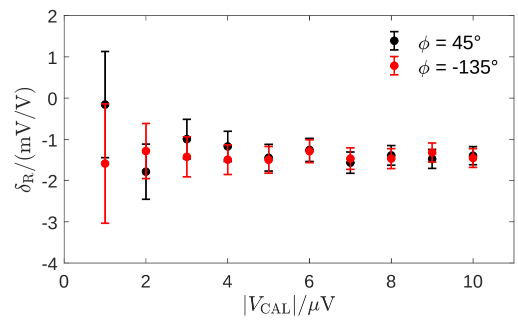

Fig. 1. Magnitude error δ_{R} for the $1\,\mathrm{mV}$ measurement range with $|V_{\mathrm{CAL}}|$ up to $10\,\mu\mathrm{V}$ at $f = 111\,\mathrm{Hz}$. To compare the outcome of this calibration with the instrument specifications, note that the DUT specified gain accuracy of $1\,\%$ would be $10\,\mathrm{mV/V}$ on this plot.

with a resistive voltage divider (RVD) to yield the calibration signal

$$V_{\mathrm{CAL}} = k_{\mathrm{IVD}} k_{\mathrm{RVD}} V_{\mathrm{S}} \mathrm{e}^{\mathrm{j}\phi}, \tag{1}$$

where k_{IVD} is the ratio of the IVD, k_{RVD} is the ratio of the RVD and ϕ represents the phase between REF and V_{CAL}. The IVD has a programmable ratio $k_{\mathrm{IVD}} = 0, 0.01, \ldots, 0.1$. The RVD is composed of resistors $R_1 = 100\,\mathrm{k\Omega}$ and $R_2 = 10\,\Omega$ yielding $k_{\mathrm{RVD}} = 10^{-4}$. The combined ratio allows for a magnitude of V_{CAL} up to $10\,\mu\mathrm{V}$. The reference signal REF drives the reference input of the DUT. The magnitude error δ_{R} of the DUT relative to V_{CAL} is defined as

$$\delta_{\mathrm{R}} = \frac{|V_{\mathrm{CAL}}^{\mathrm{read}}| - |V_{\mathrm{CAL}}|}{|V_{\mathrm{CAL}}|}, \tag{2}$$

where $V_{\mathrm{CAL}}^{\mathrm{read}}$ is the value of V_{CAL} measured by the DUT.

For these measurements, the DUT input filter was set to the 4th order with time constant $T_{\mathrm{C}} = 136\,\mathrm{ms}$. For each V_{CAL} measurement point, $V_{\mathrm{CAL}}^{\mathrm{read}}$ was sampled with the DUT at a frequency of $2\,\mathrm{Hz}$, while at the same time $\mathrm{V_S}$ was sampled by means of a 3458A voltmeter in ACV SYNC sampling mode. Each measurement took approximately $150\,\mathrm{s}$, making available about 50 readings of V_{S} and 300 readings of $V_{\mathrm{CAL}}^{\mathrm{read}}$ per calibration point to estimate the type A uncertainty. Fig. 1 reports the magnitude error δ_{R} for $|V_{\mathrm{CAL}}|$ ranging from $1\,\mu\mathrm{V}$ to $10\,\mu\mathrm{V}$ at a frequency of $111\,\mathrm{Hz}$, with phase shifts $\phi = 45°$ and $\phi = -135°$. The bars represent the combined expanded uncertainty ($k = 2$), dominated by the type A component.

III. Noise Response

The knowledge of the noise response of an LIA is usually necessary in the evaluation of the uncertainty of measuring systems employing LIAs, either as zero detectors or as vector meters. Reference [8] reports a detailed analysis, both theoretical and experimental, of the Allan variance of an LIA with moving-average filter up to the fourth order when the input is driven by a white noise source. The ZI MFLI operates instead with an autoregressive (AR) filter up to the eighth order [6], and its noise response is analyzed here. In general, the output from each LIA channel is recorded with sampling frequency f_s and period $T_\mathrm{s} = 1/f_\mathrm{s}$. Let us represent the samples recorded from channel X by the time series X_k, k integer, and let $S_X(f)$ be its one-sided spectral density function. The Allan variance of the X_k's is given by [9]

$$\sigma^2_{\bar{X}}(\tau_j) = 2\int_0^{f_\mathrm{s}/2} \frac{\sin^4(\pi f \tau_j)}{(\tau_j/T_\mathrm{s})^2 \sin^2(\pi f)} S_X(f)\,\mathrm{d}f, \tag{3}$$

$$= 2\int_0^{f_\mathrm{s}/2} \frac{\sin^4(\pi f \tau_j)}{(\tau_j/T_\mathrm{s})^2 \sin^2(\pi f)} |H(f)|^2 S_X^{\mathrm{in}}(f)\,\mathrm{d}f. \tag{4}$$

where $H(f)$ is the LIA filter transfer function, $S_X^{\mathrm{in}}(f)$ is the spectral density function of the X component of the noise at the input of the filter (the LIA is referenced at frequency f_ref, and f can thus be considered as an offset from f_ref) and $\tau_j = 2^j T_\mathrm{s}$, $j = 0, 1, 2, \ldots$, is the averaging time, for simplicity assumed to be a power of two of the sampling period. For an AR(n) filter of order n with coincident poles and time constant T_n, the transfer function is

$$H(f) = \left(\frac{1 - \mathrm{e}^{-T_\mathrm{s}/T_\mathrm{n}}}{1 - \mathrm{e}^{-T_\mathrm{s}/T_\mathrm{n}} \mathrm{e}^{-2\mathrm{i}\pi f T_\mathrm{s}}}\right)^n. \tag{5}$$

If the LIA input is driven by the white noise generated by a resistor R at thermodynamic temperature T, $S_X^{\mathrm{in}}(f) = 4k_\mathrm{B}TR$, where k_B is the Boltzmann constant. The integral in (4) together with (5) can be solved numerically.

Fig. 2 reports the computed and measured Allan deviations of the LIA X channel for the filters of order 1 and 8, with $f_\mathrm{ref} = 400\,\mathrm{Hz}$, $T_\mathrm{n} \approx 0.9982\,\mathrm{s}$ and $f_\mathrm{s} \approx 104.6\,\mathrm{Hz}$, when the input is driven by the white noise generated by a $100\,\mathrm{k\Omega}$ resistor at about $26\,^\circ\mathrm{C}$, with $S_X^{\mathrm{in}}(f) \approx 1.64 \times 10^{-15}\,\mathrm{V^2/Hz}$ (the effect of the LIA input noise, whose spectral density function is about $6.3\times10^{-18}\,\mathrm{V^2/Hz}$ above $1\,\mathrm{kHz}$, is practically negligible). The sampling frequency is such that the filter output is sampled with negligible aliasing. The solid lines represent the theoretical Allan deviations computed according to (4). The circles with uncertainty bars represent the values estimated from the measurements. These values and their uncertainties were determined from the estimated values of the *Haar wavelet variance*, according to the relationship between the Allan variance and the Haar wavelet variance described in [10]. The dashed line represents the Allan deviation expected for an unfiltered white noise of the same level. As can be seen, the measured values are compatible with the theoretical values. The Allan deviation behaviour shown in Fig. 2 is typical of an LIA: for τ much less than T_C, the Allan deviation, and hence the type A uncertainty, increases because the readings are strongly correlated; at higher τ, the readings become uncorrelated and the Allan deviation follows the behaviour for white noise. For Fig. 1, T_s and τ are such that the Allan deviation follows the white noise behaviour.

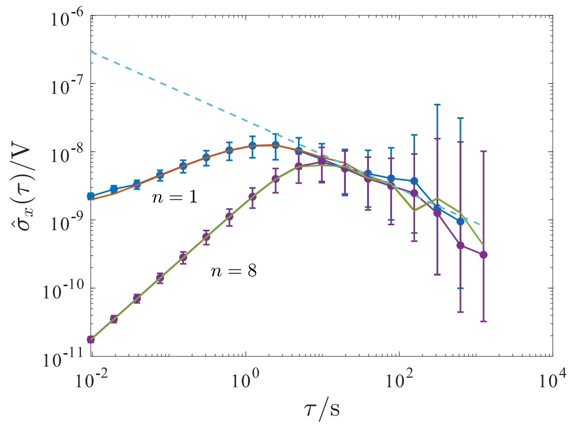

Fig. 2. Calculated (solid lines) and measured Allan deviations of the DUT X channel for the filters of order 1 and 8 (the parameters are given in the text), when the input is driven by white noise. The dashed line represents the Allan deviation of the unfiltered white noise.

IV. Acknowledgments

This work has been supported by the project CAPSTAN *Quantum electrical Italian national capacitance standard* funded by the MIUR *Progetti di Ricerca di Rilevante Interesse Nazionale* (PRIN) Bando 2020, grant 2020A2M33J.

V. Conclusion

We reported a rather simple method to improve the magnitude error of an LIA (in this case by about a factor of 10) and the analysis of the noise response of the instrument with respect to its filter transfer functions. At the conference we will present the calibration of δ_R at frequency up to $10\,\mathrm{kHz}$ (including phase effects on both the AC source and the voltage dividers) and a more detailed derivation of the Allan deviation in different operating conditions (e.g. for different $T_\mathrm{s}/T_\mathrm{n}$ and in presence of aliasing).

References

[1] D. Corminboeuf, "Calibration of the absolute linearity of lock-in amplifiers," *IEEE Trans. Instrum. Meas.*, vol. 68, pp. 2060–2065, 2019.

[2] A. Cultrera *et al.*, "A new calibration setup for lock-in amplifiers in the low frequency range and its validation in a bilateral comparison," *Metrologia*, vol. 58, p. 025001, 2021.

[3] D. Georgakopoulos, I. F. Budovsky, and S. P. Benz, "Evaluation of a Josephson arbitrary waveform synthesizer at low voltages for the calibration of lock-in amplifiers," *IEEE Trans. Instrum. Meas.*, vol. 70, pp. 1–7, 2021.

[4] EURAMET Project n. 1466, "Calibration of lock-in amplifiers," 2019. [Online]. Available: www.euramet.org

[5] *Model SR850 DSP Lock-In Amplifier User Manual*, 2nd ed., Stanford Research System, Jan 2009. [Online]. Available: thinksrs.com

[6] Zurich Instruments AG. MFLI user manual. [Online]. Available: https://docs.zhinst.com/mfli_user_manual

[7] J. Nissilä *et al.*, "A precise two-channel digitally synthesized ac voltage source for impedance metrology," in *2014 Conference on Precision Electromagnetic Measurements*, 2014, pp. 768–769.

[8] T. J. Witt and N. E. Fletcher, "Standard deviation of the mean and other time series properties of voltages measured with a digital lock-in amplifier," *Metrologia*, vol. 47, pp. 616–630, 2010.

[9] D. B. Percival, "Characterization of frequency stability: frequency-domain estimation of stability measures," *Proc. IEEE*, vol. 79, pp. 961–972, 1991.

[10] ——, "A wavelet perspective on the Allan variance," *IEEE Trans. Ultrason. Ferroelectr. Freq. Control*, vol. 63, pp. 538–554, 2016.